AUTOMATIC DETECTION OF CEREBRAL MICROBLEEDS VIA DEEP LEARNING BASED 3D FEATURE REPRESENTATION

Hao Chen[1,*] *Lequan Yu*[2,*] *Qi Dou*[1] *Lin Shi*[3,4] *Vincent CT Mok*[3] *Pheng Ann Heng*[1,5]

[1] Department of Computer Science and Engineering, The Chinese University of Hong Kong
[2] Department of Computer Science and Technology, Zhejiang University, China
[3] Department of Medicine and Therapeutics, The Chinese University of Hong Kong
[4] Chow Yuk Ho Technology Center for Innovative Medicine, The Chinese University of Hong Kong
[5] Shenzhen Institute of Advanced Technology, Chinese Academy of Sciences, China

ABSTRACT

Clinical identification and rating of the cerebral microbleeds (CMBs) are important in vascular diseases and dementia diagnosis. However, manual labeling is time-consuming with low reproducibility. In this paper, we present an automatic method via deep learning based 3D feature representation, which solves this detection problem with three steps: candidates localization with high sensitivity, feature representation, and precise classification for reducing false positives. Different from previous methods by exploiting low-level features, e.g., shape features and intensity values, we utilize the deep learning based high-level feature representation. Experimental results validate the efficacy of our approach, which outperforms other methods by a large margin with a high sensitivity while significantly reducing false positives per subject .

Index Terms— cerebral microbleeds, feature representation, deep learning, object detection

1. INTRODUCTION

Cerebral microbleeds (CMBs) are small haemorrhages of blood vessels in the brain, which are prevalent in the elderly population. As shown in Fig. 1, they appear as hypointense, rounded and sporadic lesions in susceptibility weighted imaging (SWI) scans. Recently, CMBs have been recognized as an important biomarker of neurovascular pathology by providing evidence of microvascular damage and leakiness [1]. Identifying the incidence of CMBs could help to assess the risk of intracerebral hemorrhage [2] and reveal the etiopathogenesis of cerebrovascular disease and neurodegenerative dementia, e.g., Alzheimer's disease [3].

The clinical manual labeling method is time-consuming and subjective with limited reproducibility. Therefore, the development of automatic detection methods would improve the pathological examination efficiency and reliability. However, this is challenging since CMB mimics (e.g., susceptibility artifacts, vein tissues and calcification) carrying similar morphological appearance could cause many false positive predictions in the detection process [1].

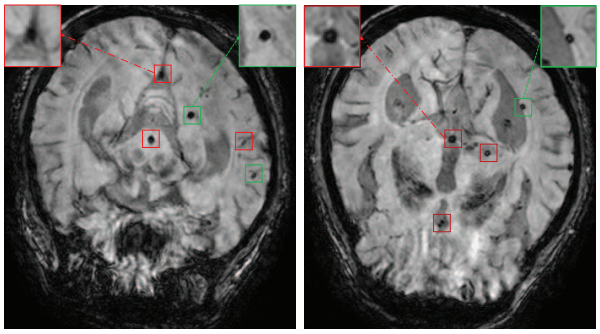

Fig. 1. Examples of true CMBs (green rectangles) and CMB mimics (red rectangles).

Many researchers have been working on this challenging problem. Seghier *et al.* [4] developed a detection method using automated segmentation and mixtures of Gaussians. Barnes *et al.* [5] presented a semi-automatic method to identify CMBs from other hypointensities in SWI by using the support vector machine (SVM). Bian *et al.* [6] proposed to locate potential CMB candidates with 2D fast radial symmetry transform (RST), followed by removing false positives (FPs) with geometric feature examination. Fazlollahi *et al.* [7] utilized a novel cascade of random forest (RF) classifiers trained on Randon transform based features to detect CMBs. One main limitation of previous methods is that they only consider low-level features including shape, compactness and size for CMBs detection, and may need a post manual review process for eliminating the large number of FPs.

Recently, deep learning has made breakthroughs in object detection with powerful feature representation in different domains [8, 9, 10, 11]. However, it has not been well explored on anatomy detection in 3D medical image modalities, e.g., SWI. In this paper, we propose to automatically detect the microbleeds in SWI by taking advantage of the deep learning

∗ Authors contributed equally.

978-1-4799-2374-8/15/$31.00 ©2015 IEEE

based 3D feature representation.

2. METHOD

The pipeline of our proposed detection framework consists of three steps: CMB candidates localization, feature representation and classification. For the first step, the CMB candidates are located with high sensitivity by statistical thresholding. Then the deep convolutional neural network (CNN) is utilized for hierarchical 3D feature representation. Finally, the SVM classifier is trained on the features to distinguish true CMBs and CMB mimics. This step can improve the precision of detection by reducing a large number of false positives while preserving high sensitivity.

2.1. CMB candidates localization

We first analyse the intensity distribution of CMBs on normalized scans, then a binary image is produced by setting a statistical threshold. The center c_n of each candidate is obtained as the centroid of 3D growing connected component. Furthermore, connected components with unrealistic large or small size are removed. Using statistical threshold method can easily remove a large number of regions, which are obviously not CMBs. Thus each candidate is represented as a 3D volume $x_n \in \mathbb{R}^{s_1 \times s_2 \times s_3}$ centered at c_n.

2.2. Deep learning based 3D feature representation

Deep CNN has been successful in object recognition with powerful feature representation when large amounts of data are available. However, direct adoption of CNN with 2D convolutional filters in 3D medical imaging modalities could face the risk of over-fitting. Because more input channels of the third dimension could introduce more weights in the neural network compared to less input channels, e.g., RGB image (3 channels). Moreover, limited available data can degrade the performance, especially in medical domain. Based on these analyses, we propose to extract the deep hierarchical high-level features from 2D (transverse plane) MRI slices $x_n^i \in I^{s_1 \times s_2}$ $(i = 1, 2, ..., s_3)$, then concatenate them as 3D feature representation, as shown in Fig. 2. It aims at increasing the number of training samples and reducing the number of parameters in neural network. In order to train such a CNN extractor, 2D slices of ground truth are extracted as the positive samples and negative samples are randomly selected away from ground truths more than $10\ mm$. The parameters $\theta = \{W, b\}$ of weight and bias in CNN are trained by minimizing the following loss function of negative log likelihood.

$$\mathcal{L}(I_j, y_j; \theta) = -y_j \log p_j - (1 - y_j) \log(1 - p_j) \quad (1)$$

$$\hat{\theta} = \arg\min_{\theta} \sum_{j=1}^{M} \mathcal{L}(I_j, y_j; \theta) \quad (2)$$

where p_j is the output posterior probability of CNN given the j^{th} input I_j, $y_j \in \{0, 1\}$ is the corresponding ground truth and M is the number of training samples. In order to improve the generalization ability, the strategies of data augmentation and dropout [12] are implemented in the training process for regularization. Ultimately, the third dimensional information of one volume sample x_n is complemented by concatenating the extracted features in consecutive slices x_n^i, as shown in Eq. 4.

$$f_n^i = g(x_n^i, \hat{\theta}),\ x_n^i \in I^{s_1 \times s_2}, i = 1, ..., s_3 \quad (3)$$

$$f_n = C\{f_n^1, ..., f_n^{s_3}\} \quad (4)$$

where f_n^i is the extracted feature vector of input x_n^i via deep compositional non-linear function $g(x_n^i, \hat{\theta})$, which is the neuron activations in the penultimate layer of CNN and f_n is the 3D feature representation after concatenation operation C.

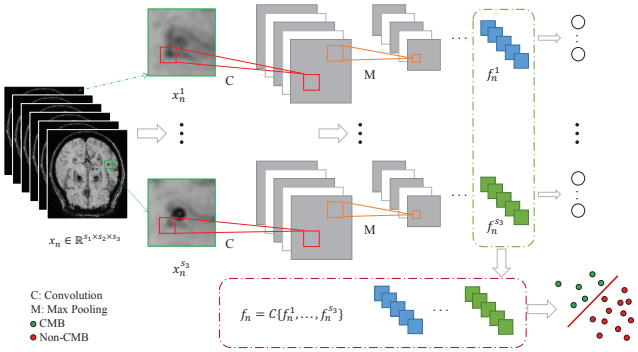

Fig. 2. The overview of 3D feature representation.

2.3. Classification with 3D feature representation

To remove the large number of FP CMBs effectively, a SVM classifier [13] is trained with L_2 regularization on proposed 3D feature representation f_n, as shown in Eq. 5.

$$\arg\min_{w} \frac{1}{2} w^T w + \lambda \sum_{n=1}^{N} max(0, 1 - w^T t_n f_n)^2 \quad (5)$$

where t_n is the ground truth for 3D sample x_n, N is the number of training samples and λ is the regularization constant.

3. EXPERIMENTS AND RESULTS

3.1. Materials and data preprocessing

The data set contains a total of 117 CMBs from 20 elderly subjects (mean age 78.6) with transient ischemic attack (TIA). SWI images were acquired on a 3.0T Philips Medical System with following parameters: volume size $512 \times 512 \times 150$, in-plane resolution $0.45 \times 0.45\ mm^2$, $2\ mm$ slice thickness and $1\ mm$ slice spacing. The ground truth was labelled by experienced neuroradiologists. The whole data set was divided into

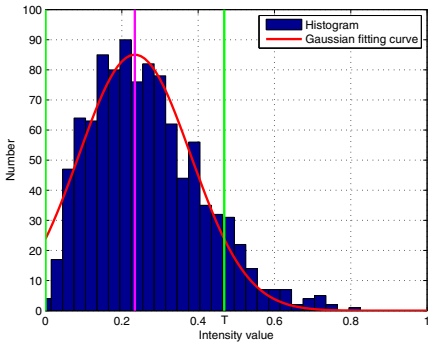

Fig. 3. Intensity value distribution of CMB.

two sections for training and testing (5 patients with a total of 55 CMBs), respectively. In the preprocessing step, the image intensity range of each patient was normalized to [0, 1], as shown in Eq. 6.

$$V' = \frac{V - V_{min}}{V_{max} - V_{min}} \tag{6}$$

where V is the original volume data and V' is the normalized volume data. Note that the V_{max} is the maximum intensity after trimming the top 1% intensity values for consistence. For the training process, the positive samples were acquired according to the ground truth labelled with experienced experts. And the negative samples were randomly selected in the image which are not overlapped with the ground truth. The size of each sample was $16 \times 16 \times 9$. Since the CMB is invariant to rotation and translation, additional positive training samples were augmented by rotating $\phi \in \{90 * k\}^\circ, k = 1 \sim 3$ and translating $d = 1 \sim 4$ voxels around the ground truth.

3.2. CMB candidates localization

In order to locate the CMB candidates, a binary image was produced by setting the threshold $T = 0.468$ after analyzing the intensity value distribution of CMB, as shown in Fig. 3. The unrealistic large components were removed after 3D region growing. This step can achieve a high recall with 95.65% while removing most of redundant regions. However, it sacrificed with a large number of FPs (more than 800 per subject).

3.3. Quantitative evaluation and comparison

We compared the performance of our approach with the methods of CNN and RF. Noting that different from the proposed approach, the input of CNN method was direct 3D volume data. It was trained with stochastic gradient descent by minimizing the loss function of negative log likelihood. For the method of RF, the training samples were first input into the RF for classification with negative training samples randomly selected. Since the random negative samples may not be representative, we added the FP samples which had been predicted by the first RF classifier into the training samples and re-trained the RF classifier, which performed better than the first classifier.

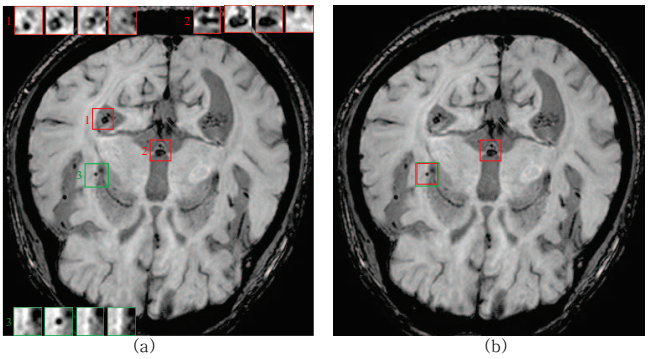

Fig. 4. Example of CMB detection: (a) RF, (b) our method (green rectangles for CMBs, red rectangles for positive predictions of each method).

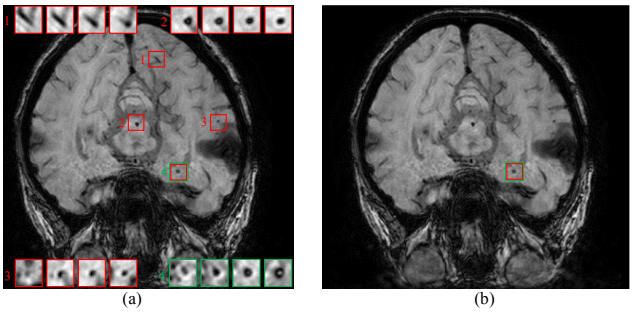

Fig. 5. Example of CMB detection: (a) CNN, (b) our method (green rectangles for CMBs, red rectangles for positive predictions of each method).

From the results of different methods shown in Table 1, we can see that our framework can outperform other methods by a large margin with less number of FPs while preserving high sensitivity (or recall). Some detection examples and transverse slices with two-interval in each example are shown in Fig. 4 and Fig. 5. The performance of Precision-Recall (PR) plane in Fig. 6 proves the effectiveness of our method. For the evaluation of FPs, Free-response Receiver Operating Characteristic (FROC) curves of different methods in Fig. 7 show the sensitivity against the average number of FPs per patient, our method can achieve about 90% recall with average 6.4 FPs per subject. The FPs of our approach are mainly blood vessels, which carry the similar morphological appearance with true CMBs. Overall, our approach generally took

Table 1. The results of different methods

Method	Sensitivity	Precision	F1-score	Average FPs
RF	0.8696	0.3540	0.5031	14.6
CNN	0.8696	0.3922	0.5405	12.4
Ours	**0.8913**	**0.5616**	**0.6891**	**6.4**

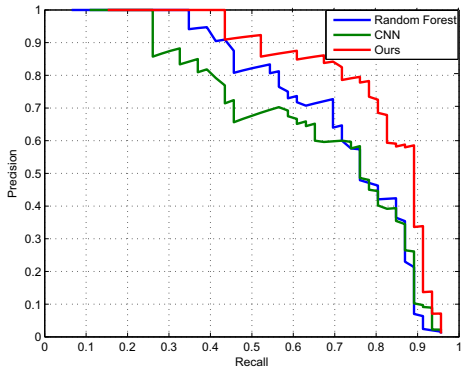

Fig. 6. Performance of different methods in PR plane.

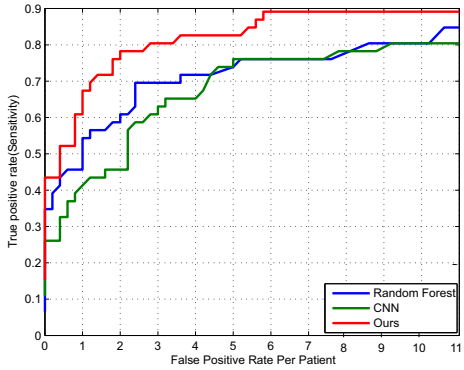

Fig. 7. Comparison of FROC curves of different methods.

less than 20 seconds for detecting the CMBs from one patient using a laptop with a 2.60 GHz Intel(R) i5-4278U CPU.

4. CONCLUSIONS

In this paper, we propose an automatic method for CMB detection with deep learning based 3D feature representation. Feature representation encoding high-level information can benefit the classification between CMB and its mimics. Experiments on clinical data validated the efficacy of our approach. In the future, we will apply it in clinical practice and compare its performance with experienced neuroradiologists.

5. ACKNOWLEDGEMENTS

The work described in this paper was supported by National Basic Research Program of China, 973 Program (Project No. 2015CB351706), Research Grants Council of Hong Kong Special Administrative Region, China (Project No. CUHK 14113214 and 412412), Natural Science Foundation of Guangdong (Project No. S2013010014973) and Chow Yuk Ho Technology Center for Innovative Medicine, The Chinese University of Hong Kong.

6. REFERENCES

[1] Andreas Charidimou and David J Werring, "Cerebral microbleeds and cognition in cerebrovascular disease: an update," *Journal of the neurological sciences*, vol. 322, no. 1, pp. 50–55, 2012.

[2] Zhaolu Wang, Yannie OY Soo, and Vincent CT Mok, "Cerebral microbleeds is antithrombotic therapy safe to administer?," *Stroke*, vol. 45, no. 9, pp. 2811–2817, 2014.

[3] Andreas Charidimou, Anant Krishnan, David J Werring, and H Rolf Jäger, "Cerebral microbleeds: a guide to detection and clinical relevance in different disease settings," *Neuroradiology*, vol. 55, no. 6, pp. 655–674, 2013.

[4] Mohamed L Seghier, Magdalena A Kolanko, Alexander P Leff, Hans R Jäger, Simone M Gregoire, and David J Werring, "Microbleed detection using automated segmentation (midas): a new method applicable to standard clinical mr images," *PloS one*, vol. 6, no. 3, pp. e17547, 2011.

[5] Samuel RS Barnes, E Mark Haacke, Muhammad Ayaz, Alexander S Boikov, Wolff Kirsch, and Dan Kido, "Semiautomated detection of cerebral microbleeds in magnetic resonance images," *Magnetic resonance imaging*, vol. 29, no. 6, pp. 844–852, 2011.

[6] Wei Bian, Christopher P Hess, Susan M Chang, Sarah J Nelson, and Janine M Lupo, "Computer-aided detection of radiation-induced cerebral microbleeds on susceptibility-weighted mr images," *NeuroImage: clinical*, vol. 2, pp. 282–290, 2013.

[7] Amir Fazlollahi, Fabrice Meriaudeau, Victor L Villemagne, Christopher Rowe, Paul Yates, Olivier Salvado, Pierrick T Bourgeat, et al., "Efficient machine learning framework for computer-aided detection of cerebral microbleeds using the radon transform," in *Proceedings of the IEEE-ISBI conference*, 2014.

[8] Alex Krizhevsky, Ilya Sutskever, and Geoffrey E Hinton, "Imagenet classification with deep convolutional neural networks," in *Advances in neural information processing systems*, 2012, pp. 1097–1105.

[9] Christian Szegedy, Wei Liu, Yangqing Jia, Pierre Sermanet, Scott Reed, Dragomir Anguelov, Dumitru Erhan, Vincent Vanhoucke, and Andrew Rabinovich, "Going deeper with convolutions," *arXiv preprint arXiv:1409.4842*, 2014.

[10] Hao Chen, Dong Ni, Xin Yang, Shengli Li, and Pheng Ann Heng, "Fetal abdominal standard plane localization through representation learning with knowledge transfer," in *Machine Learning in Medical Imaging*, pp. 125–132. Springer, 2014.

[11] Cewu Lu, Hao Chen, Qifeng Chen, Hei Law, Yao Xiao, and Chi-Keung Tang, "1-hkust: Object detection in ilsvrc 2014," *arXiv preprint arXiv:1409.6155*, 2014.

[12] Geoffrey E Hinton, Nitish Srivastava, Alex Krizhevsky, Ilya Sutskever, and Ruslan R Salakhutdinov, "Improving neural networks by preventing co-adaptation of feature detectors," *arXiv preprint arXiv:1207.0580*, 2012.

[13] Chih-Chung Chang and Chih-Jen Lin, "LIBSVM: A library for support vector machines," *ACM Transactions on Intelligent Systems and Technology*, vol. 2, pp. 27:1–27:27, 2011, Software available at `http://www.csie.ntu.edu.tw/~cjlin/libsvm`.